Cryptospirolepine, a Unique Spiro-nonacyclic Alkaloid Isolated from Cryptolepis sanguinolenta

Albert N. Tackie, Gilbert L. Boye, Maged H. M. Sharaf, Paul L. Schiff Jr., Ronald C. Crouch, Timothy D. Spitzer, Robert L. Johnson, John Dunn, Doug Minick, and Gary E. Martin

J. Nat. Prod., **1993**, 56 (5), 653-670• DOI:
10.1021/np50095a001 • Publication Date (Web): 01 July 2004

Journal of Natural Products
Vol. 56, No. 5, pp. 653-670, May 1993

CRYPTOSPIROLEPINE, A UNIQUE SPIRO-NONACYCLIC ALKALOID ISOLATED FROM *CRYPTOLEPIS SANGUINOLENTA*

ALBERT N. TACKIE, GILBERT L. BOYE,

Centre for Scientific Research into Plant Medicine, Mampong-Akwapim, Ghana

MAGED H.M. SHARAF, PAUL L. SCHIFF JR.,

Department of Pharmaceutical Sciences, School of Pharmacy, University of Pittsburgh, Pittsburgh, Pennsylvania 15261

RONALD C. CROUCH, TIMOTHY D. SPITZER, ROBERT L. JOHNSON, JOHN DUNN, DOUG MINICK, and GARY E. MARTIN*

Division of Organic Chemistry, Burroughs Wellcome Company, Research Triangle Park, North Carolina 27709

ABSTRACT.—From the alkaloidal fractions of the West African plant *Cryptolepis sanguinolenta* (Asclepiadaceae), two alkaloids were purified: one was identified as the known indoloquinoline alkaloid cryptolepine [**1**]. A second, novel alkaloid was shown to have an empirical formula of $C_{34}H_{24}N_4O$ based on exact mass measurement. Through the concerted application of a series of homonuclear and inverse-detected 2D nmr experiments, the structure of the second alkaloid was established as a spiro-nonacyclic alkaloid, cryptospirolepine. One portion of the structure of cryptospirolepine [**2**] may be biogenetically derived from cryptolepine [**1**].

Cryptolepis sanguinolenta (Lindl.) Schlechter (Asclepiadaceae), a shrub indigenous to West Africa, has long been employed by Ghanaian traditional healers in the treatment of various fevers, including malaria (1). A root decoction has been used in the clinical therapy both of malaria and of urinary and upper respiratory tract infections by Oku Ampofo at the Centre for Scientific Research into Plant Medicine in Ghana since 1974 (1). The indoloquinoline alkaloid cryptolepine (5-methyl-5*H*-indolo-[3,2-*b*]-quinoline) [**1**] was first isolated from extracts of the roots of *Cryptolepis triangularis* N. E. Br., a species native to the Belgian Congo, by Clinquart in 1929 (2). Shortly thereafter, the alkaloid was again isolated from the same species by Delvaux (3). Quite paradoxically, cryptolepine had been synthesized some 20 years prior by Fichter and coworkers (4–6). Cryptolepine was isolated from a Nigerian sample of *Cr. sanguinolenta* in 1951 by Gellert *et al.* (7). Almost 30 years later, the alkaloid was isolated from a Ghanaian sample of *Cr. sanguinolenta* by Dwuma-Badu *et al.* (8), along with quindoline (norcryptolepine) and a partially characterized alkaloid (CSA-3). Finally, cryptolepine was most recently isolated from this same Ghanaian variant in 1990 by Ablordeppey *et al.* (9).

Cryptolepine [**1**] has been found to possess several interesting pharmacological activities. Almost 60 years ago, Raymond-Hamet (10) reported that administration of cryptolepine HCl to dogs at a dosage of 15–30 mg/kg produced marked hypothermia and decreased the hypertensive and renal vasoconstrictive actions of epinephrine. Furthermore, ip injection (120 mg/kg) of the compound was lethal to guinea pigs in about 12 h (10). In addition, Raymond-Hamet (11) observed that iv administration (5 mg/

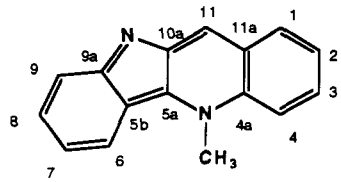

1

kg) of the alkaloid produced a marked and protracted hypotensive response in the vagotomized dog with a corresponding decrease in renal volume. These effects were apparently in response to the pronounced vasodilatation produced by the alkaloid. Boakye-Yiadom (12) observed in 1979 that extracts of the roots of *Cr. sanguinolenta* were found to inhibit the growth of *Neisseria gonorrhoeae, Escherichia coli,* and *Candida albicans*, but not of *Pseudomonas aeruginosa*. Cryptolepine HCl was found to possess antimicrobial activity against a number of Gram-positive and Gram-negative pathogens (13). A detailed study of the effects of cryptolepine HCl on the microbial kinetics and growth of *Staphylococcus aureus* demonstrated that the alkaloid possesses both bacteriostatic and bactericidal actions (14). In a series of experiments in the last decade, Bamgbose and Noamesi (15) reported that cryptolepine possesses hypotensive, anti-inflammatory, antibacterial, and vasoconstrictive activity. In addition, these same authors observed that cryptolepine HCl is a noradrenoreceptor antagonist in the isolated rat vas deferens (16) and also inhibits (ip injection; 1–20 mg/kg) carrageenan-induced hind paw edema in the rat (17).

Two high-field nmr studies of cryptolepine [**1**], the first in $CDCl_3$ (9) and the second in DMSO-d_6 (18), were recently reported. The assignments were rigorously confirmed in both studies by different, but comparable, 2D nmr techniques and were in agreement. Typically, these data form the basis for the study and structural assignment of other alkaloids under investigation in this and related species.

This paper reports the isolation of cryptolepine [**1**] and the determination of structure of a novel spiro-alkaloid, cryptospirolepine [**2**]

RESULTS AND DISCUSSION

Powdered, dried roots of *Cr. sanguinolenta* were defatted with petroleum ether and extracted with EtOH. The EtOH extract was treated with aqueous HOAc, filtered, alkalinized with NH_4OH, and extracted repeatedly with $CHCl_3$. The combined $CHCl_3$ extracts were chromatographed over Al_2O_3. Elution with petroleum ether-$CHCl_3$ (1:2) followed by elution with $CHCl_3$ gave cryptospirolepine [**2**]. Finally, elution with $CHCl_3$-EtOH (9:1) afforded cryptolepine [**1**] with a minor (ca. 5%) and apparently closely related contaminant.

Cryptospirolepine [**2**] crystallized as light brownish-pink crystals from absolute EtOH. The uv spectrum showed maxima at 506 nm (log ε 4.44), 474 (4.19), 368 (4.38), 352 (sh) (4.27), 280 (4.65), 250 (4.80), 223 (sh) (4.75), and 215 (4.83) and was thus characteristic of an indoloquinoline-based alkaloid (8). The ir spectrum (film, KBr) displayed a weak carbonyl absorption at 1612 cm^{-1} and strong aromatic bands at 1588 and 1512 cm^{-1}.

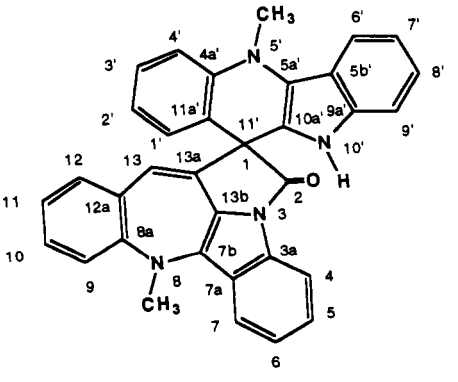

2

As the carbonyl absorbance was abnormally low at 1612 cm^{-1}, Ft-ir spectra were recorded in a series of solvents of increasing polarity.

The fabms (glycerol) of cryptospirolepine [**2**] gave an $[M + H]^+$ ion at *m/z* 505 and fragment ions between 230 and 275. The hrms of the ion at 505 Da was achieved using the method described by Johnson and Taylor (19) using oligomers of polyethylene glycol for reference masses. The measured exact mass was 505.1989 and corresponds to an empirical formula of $C_{34}H_{24}N_4O$ with an error of −3.9 mmu. Exact masses of fragment ions are given in Table 1.

TABLE 1. High-resolution Masses of Cryptospirolepine [**2**] and Fragment Ions Observed in the Fab Mass Spectrum.

Mass (Da)	Intensity (%)	Exact Mass	Δmmu	Elemental Composition
505	100	505.1989	−3.9	$C_{34}H_{25}N_4O$
233	70	233.1037	−4.2	$C_{16}H_{13}N_2$
273	20	273.1075	+4.7	$C_{18}H_{13}N_2O$
245	23	245.1082	+0.3	$C_{17}H_{13}N_2$
246	25	246.1163	+0.6	$C_{17}H_{14}N_2$
259	23	259.1201	−3.4	$C_{18}H_{15}N_2$

The relatively large errors for these measurements shown in Table 1 are the result of difficulties inherent in measuring the accurate masses of ions generated in fab spectra. For example, Figure 1 shows the peak for *m/z* 259 at a resolution of 5500. Peak A arises from the alkaloid, and its accurate mass is reported in Table 1 as 259.1201; Peak B is due to an interference ion (chemical "noise") from the glycerol matrix. Software enhancement of Peak A allowed its exact mass to be measured, albeit with somewhat reduced accuracy, even though full resolution from Peak B could not be achieved.

The ^{1}H-nmr spectrum of **2** (Figure 2) contained resonances corresponding to 24 protons. A sharp one-proton singlet resonating at 10.669 ppm was initially suspected to arise from either an -OH or -NH. Likewise, the two three-proton singlets resonating at 4.365 and 3.952 ppm could arise from *O*-Me and/or *N*-Me substituents.

The decoupled ^{13}C-nmr spectrum of **2** is shown in Figure 3. Thirty-four carbons were observed in the spectrum; 28 were vinyl or aromatic. Resonances in the ^{1}H and ^{13}C spectra were consistent with the empirical formula $C_{34}H_{24}N_4O$ derived from hrms.

The COSY spectrum of the aromatic region is shown in Figure 4, encompassing 17 proton resonances ranging from 6.27 to 8.40 ppm. Although congested, the COSY spectrum established four four-spin systems. The singlet resonating at 6.273 ppm was long-range-coupled to the proton resonating at 8.400 ppm. No additional information to relate four-spin systems to one another was obtained from a relayed-COSY (RCOSY) spectrum with $\tau = 60$ msec.

Arbitrarily, we labeled the four-spin systems A, B, C, and D. Spin system A was comprised of the protons, in sequence, resonating at 8.400, 7.459, 7.827, and 8.004 ppm. The proton at 8.400 ppm was long-range-coupled to the singlet resonating at 6.273 ppm. Spin system B involved the protons resonating at 8.324, 7.059, either the resonance at 7.012 or at 7.009, and finally 6.613 ppm. Spin system C accounted for the protons resonating at 8.094, 7.053, either the resonance at 7.012 or at 7.009, and 7.122 ppm. Finally, spin system D was comprised of the protons resonating at 6.783, 6.622, 7.202, and 7.239 ppm.

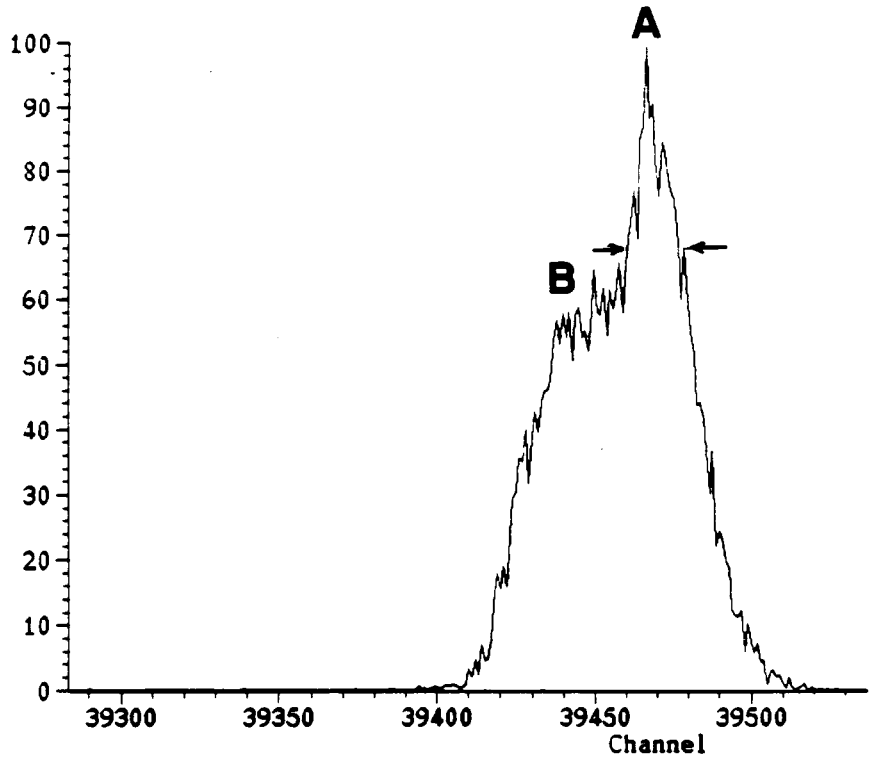

FIGURE 1. Fab mass spectrum of the 259 Da ion at a resolution of 5500. Peak A arises from a fragment ion of cryptospirolepine [**2**] with an accurate mass of 259.1201; Peak B is an interference ion from the glycerol matrix and constitutes "chemical noise."

To expand the four proton four-spin systems, which invoke four 1,2-disubstituted phenyl moieties, into more meaningful structural fragments, it was necessary to begin the concerted interpretation of data from several additional 2D nmr experiments, which included HMQC (inverse-detected heteronuclear chemical shift correlation), HMBC (long-range inverse-detected heteronuclear correlation), and ROESY. The HMQC spectrum of the aromatic region is shown in Figure 5. The carbons resonating at 188.4, 93.2, 66.0, 36.25, and 36.15 ppm are not included in the presentation. The 188.4 and 66.0 ppm resonances were quaternary carbons; the resonances at 36.25 and 36.15 ppm were *N*-Me's; finally, the carbon resonating at 93.2 ppm correlated with the one-proton singlet resonating at 6.273 ppm. The HMBC spectrum of the aromatic region is shown in Figure 6. The NOESY spectrum at 500 MHz gave no useful nOe responses; only weak NOESY responses were observed at 400 MHz, prompting the acquisiton of a ROESY spectrum. ROESY responses were utilized primarily to establish through space connectivities from the *N*-Me substituents to the peri aromatic protons.

SPIN SYSTEMS A AND B.—Returning to the protons defined as spin system A and incorporating data from the HMQC, HMBC, and ROESY spectra, we established structure **3**. The direct proton-carbon correlations were trivially established from the HMQC data. Connectivities in the HMBC spectrum allowed the completion of the benzene ring, establishing the two bridgehead carbons as resonances at 116.8 and 138.5 ppm. Based on chemical shift, the latter bears an *N*-Me, confirmed by the observation of a connectivity from the *N*-Me singlet at 4.365 ppm. Likewise, rOe's were observed from the 4.365 ppm *N*-Me to the protons resonating at 8.004 ppm and 8.324

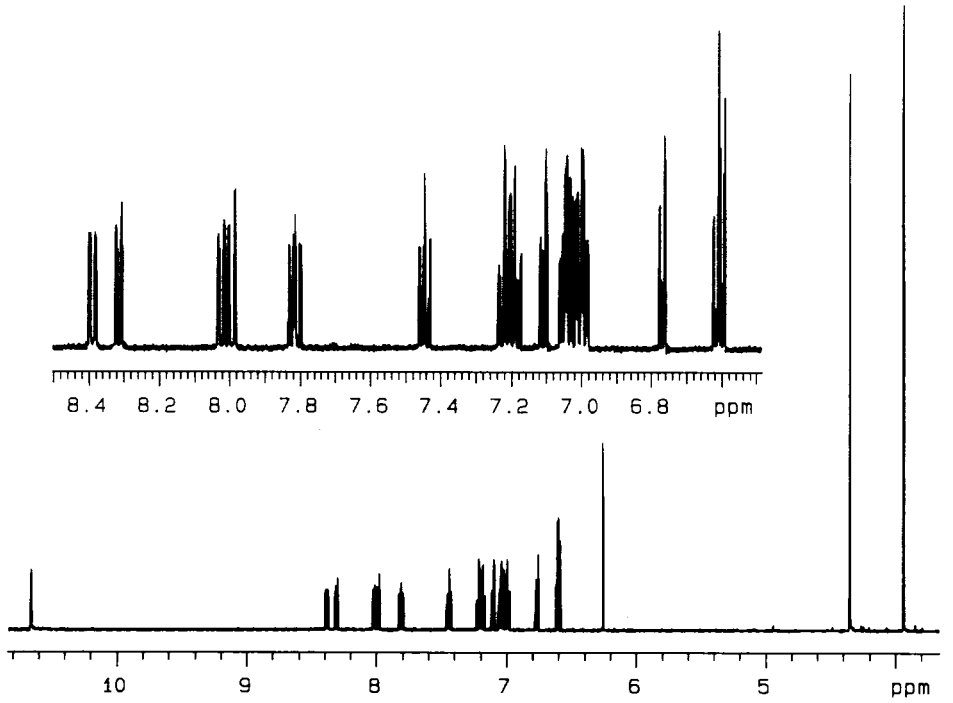

FIGURE 2. ^{1}H-nmr spectrum of cryptospirolepine [**2**] in DMSO-d_6 recorded at an observation frequency of 500 MHz. An expansion of the aromatic region, which contains resonances for 17 protons, is shown in the inset.

ppm in spin system B. A correlation was also observed from the *N*-Me to a quaternary carbon resonating at 123.4 ppm. Assuming the correlation from the 4.365 ppm *N*-Me resonance to the 123.4 ppm ^{13}C resonance to be a three-bond correlation requires the 123.4 ppm carbon to be the nitrogen-bearing quaternary carbon in the next ring. To

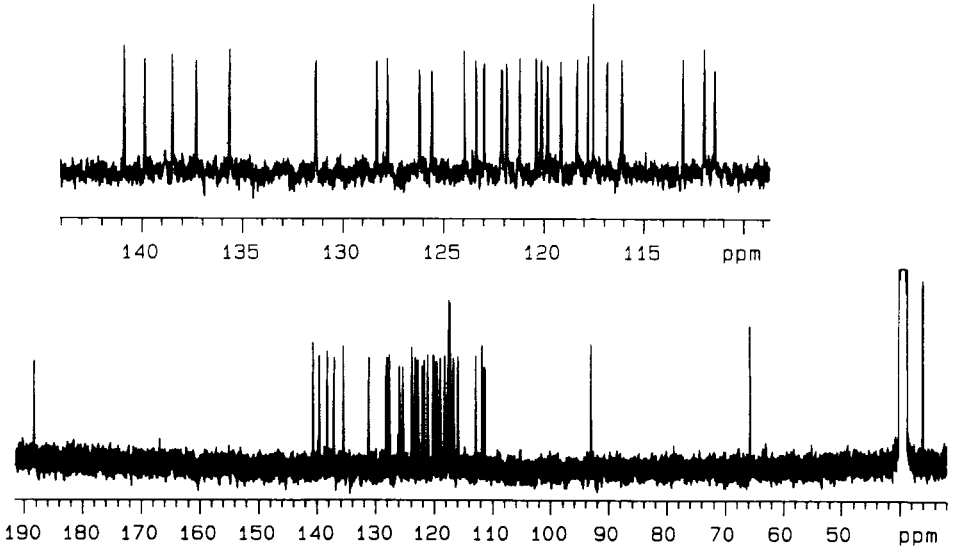

FIGURE 3. ^{13}C-nmr spectrum of cryptospirolepine [**2**] recorded in DMSO-d_6 at 100.6 MHz. An expansion of the aromatic region is presented in the inset.

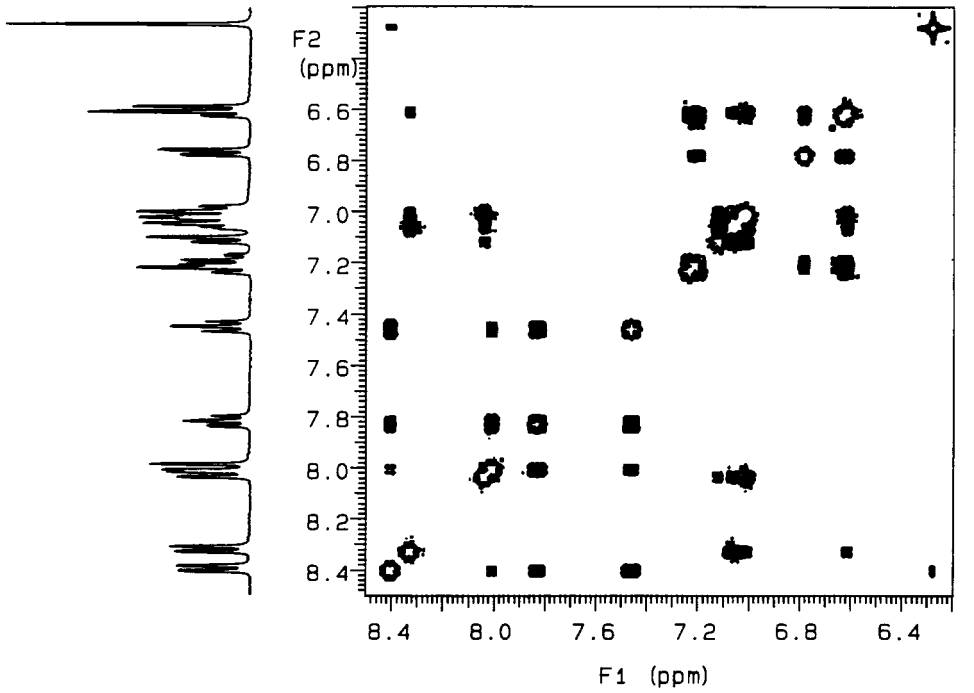

FIGURE 4. COSY spectrum of the aromatic region of the ^{1}H-nmr spectrum of cryptospirolepine [**2**] in DMSO-d_6.

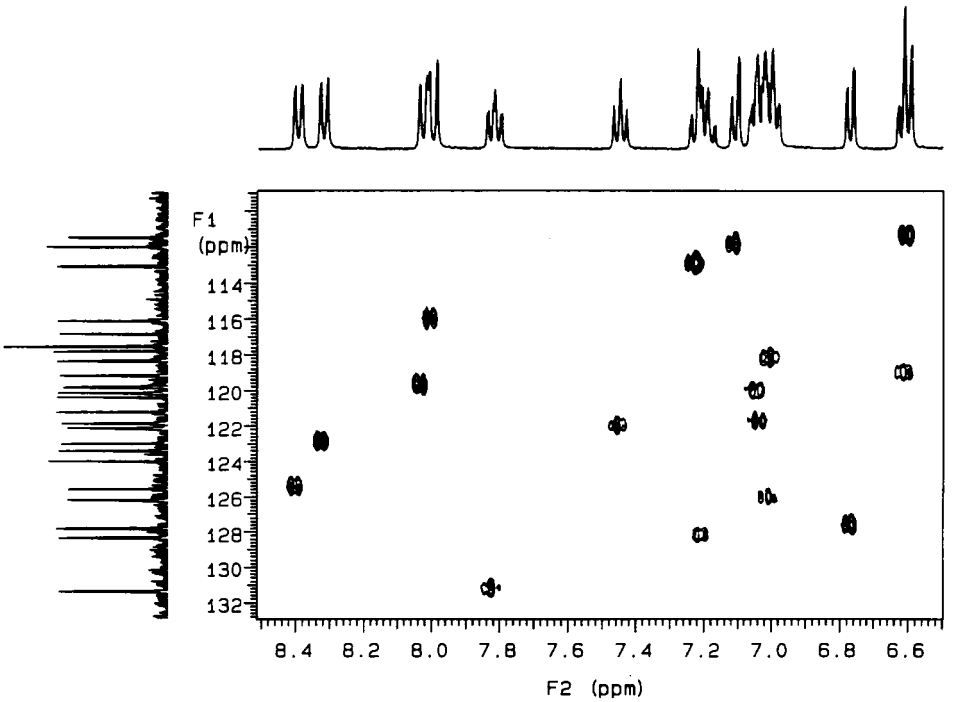

FIGURE 5. Inverse-detected heteronuclear chemical shift correlation spectrum (HMQC) of the aromatic region of cryptospirolepine [**2**] in DMSO-d_6. The protonated carbon resonating at 93.2 ppm correlated with the proton singlet resonating at 6.273 ppm. The *N*-Me resonances are also excluded from the plot.

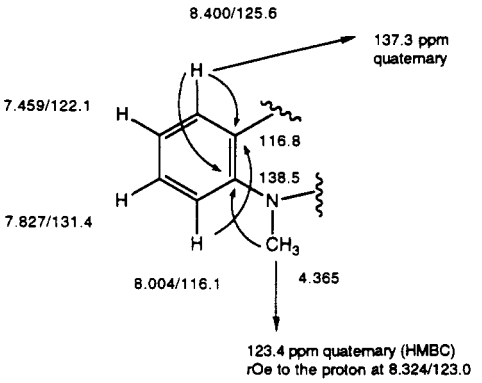

3

account for the disparity in the chemical shift of the two nitrogen-bearing quaternary carbons, the latter must have a second nitrogen located at a position beta to the position of the 123.4 ppm carbon in the molecular skeleton.

In very similar fashion, spin system B [**4**] was also assembled. The bridgehead carbon chemical shifts were 117.8 and 139.9 ppm. The latter was again suggestive of the direct attachment of a nitrogen. Several other connectivities were important. First, the 4.365 ppm *N*-Me gave a strong rOe to the proton resonating at 8.324 ppm in spin system B. The proton at 8.324 ppm was correlated via long-range coupling to the quaternary carbon resonating at 123.4 ppm. This observation established the interrelation between spin systems A and B and allowed them to be unified into a still larger substructural fragment, substructure A [**5**], discussed below.

SUBSTRUCTURE A.—The connectivities observed in association with spin systems A and B allowed the assembly of these fragments into a much larger substructural component **5**. The arrangement of the components of **5** began to assemble a structural moiety having a distinct resemblance to the indolo-*N*-methylquinoline nucleus of cryptolepine [**1**]. The chemical shift of the *N*-Me-bearing quaternary carbon at 123.4 ppm is reasonable if we invoke the relationship of this carbon beta to the indole-nitrogen atom denoted by the dashed lines of **5**.

Continuing to develop **5** further, we next considered the connectivities associated with the singlet resonating at 6.273 ppm. This resonance exhibited a long-range coupling to the 8.400 ppm proton in the COSY spectrum and a strong rOe to this same resonance. The chemical shift of the directly attached carbon, at 93.2 ppm, strongly implied vinyl rather than aromatic character. Connectivities in the HMBC spectrum link the 6.273 ppm singlet with the quaternary carbons at 116.8, 120.4, and 66.0

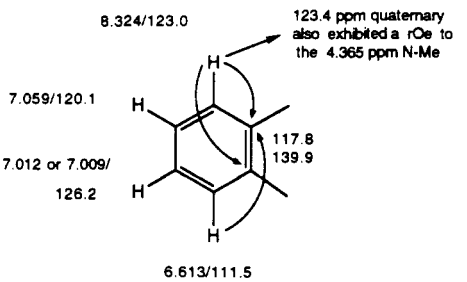

4

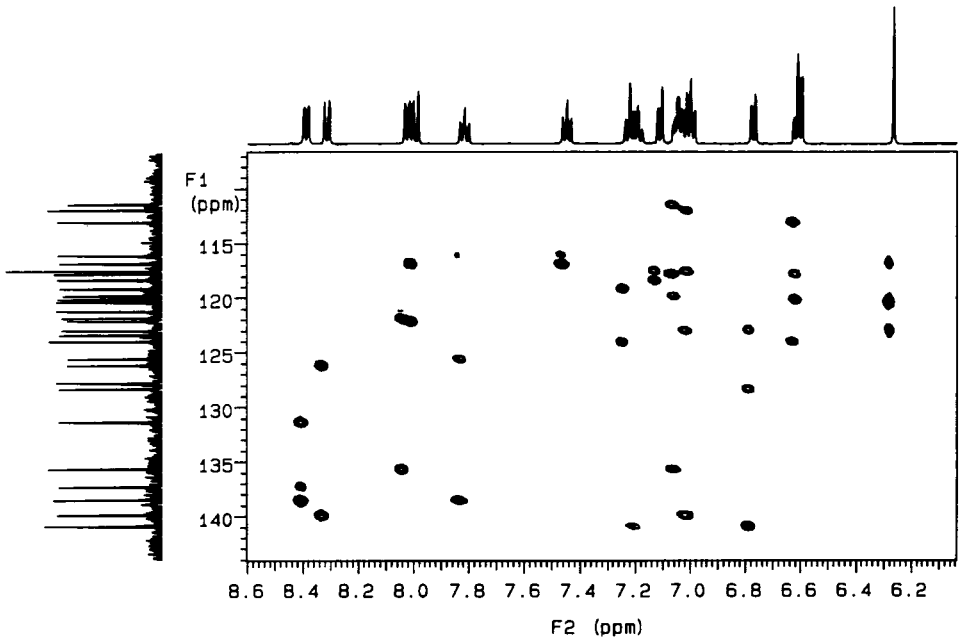

FIGURE 6. Inverse-detected long-range heteronuclear chemical shift correlation (HMBC) spectrum of cryptospirolepine [2] in DMSO-d_6. The spectrum was recorded at 500 MHz with the long-range delay optimized for 10 Hz (50 msec) and the low-pass J-filter set for an average one-bond coupling constant of 165 Hz. Data were subjected to hypercomplex Fourier transformation.

ppm. Given these observations, we may tentatively link the 6.273/93.2 proton-carbon pair directly to the quaternary carbon resonating at 116.8 ppm.

A connectivity from the 8.400 ppm proton in the HMBC spectrum to the quaternary carbon resonating at 137.3 ppm, based on the connection just made, must be attributed to a $^4J_{CH}$ long-range coupling pathway that, although uncommon, is certainly not unprecedented. The further connectivity of the 6.273 ppm proton to the 120.4 ppm quaternary carbon can also be added, giving, as shown if the dashed bonds are correct, an indolobenzazepine nucleus [**6**].

Further support for the presence of an indolobenzazepine nucleus in the structure of the alkaloid was obtained from the acquisition of a SIMBA spectrum. SIMBA or Selec-

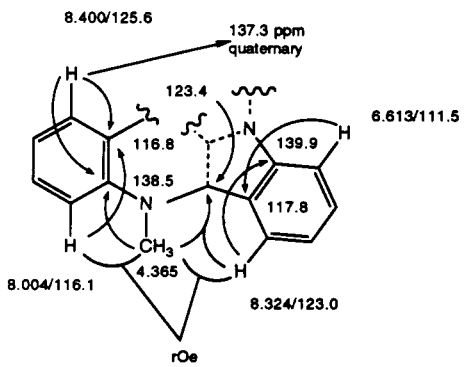

5

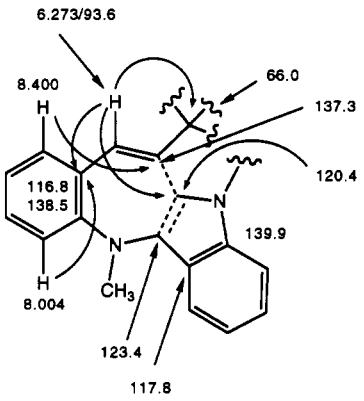

6

tive Inverse Multiple Bond Analysis, recently described by Crouch and Martin (20), is a new, proton-detected, selective one-dimensional analogue of the well-established HMBC experiment. Application of a 12-msec selective Gaussian pulse to the quaternary carbon resonating at 120.4 ppm in a SIMBA experiment gave the spectrum shown in Figure 7. As expected, the 120.4 ppm carbon was correlated with the proton resonating at 6.273 ppm. Rather than appearing as a singlet as it does in the normal proton reference spectrum, the 6.273 ppm proton was observed in the SIMBA spectrum as a 6.8 Hz doublet, the coupling arising from the heteronuclear coupling pathway selectively

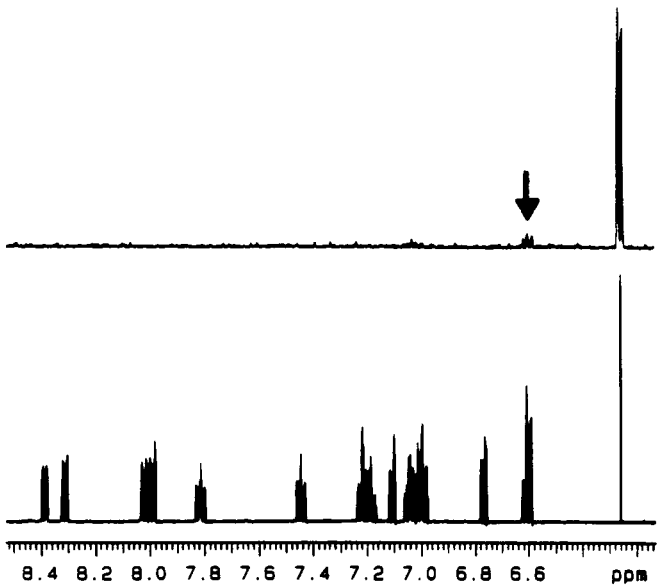

FIGURE 7. SIMBA spectrum (20) obtained at 500 MHz by the application of a 12 msec selective Gaussian pulse applied to the 120.4 ppm quaternary carbon resonance of cryptospirolepine [**2**] in DMSO-d_6. The SIMBA trace is plotted above a normal high-resolution ^{1}H-nmr spectrum. Responses were observed in the SIMBA spectrum to the proton singlet resonating at 6.273 ppm (H-13), and a weak four-bond coupling response to the proton resonating at 6.613 ppm (H-4, response denoted by arrow) was also observed. The former response was observed in the HMBC spectrum shown in Figure 6. The latter response represents new information supporting the presence of the indolo-*N*-methylbenzazepine component of the lower, pentacyclic portion of the structure of **2**.

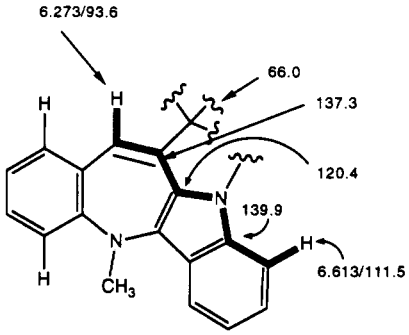

7

exploited to excite the proton resonance in the experiment. A much weaker, but far more important, response was the double doublet ($J = 8.1$, 6.3 Hz) denoted in the SIMBA spectrum by the arrow to the proton resonating at 6.613 ppm. The resonance in question was a member of the four-spin system, B, shown by **4** (see also substructure A [**5**]) and normally appeared as a simple doublet. The response denoted by the arrow in the SIMBA spectrum shown in Figure 7 must therefore arise via a four-bond coupling ($^4J_{CH}$) between the proton resonating at 6.613 ppm and the 120.4 ppm quaternary carbon. These connectivities are shown by the darkened bonds of **7** and further substantiate the presence of the indolobenzazepine structure.

The substituent occupying the remaining valence site of the indole nitrogen of **6** and **7** remained to be explained. Based on the observed connectivity from the 6.273 ppm proton to the aliphatic quaternary carbon resonating at 66.0 ppm, it is probable that this carbon is linked to the 137.3 ppm quaternary carbon of the azepine ring.

SPIN SYSTEMS C AND D.—In a fashion analogous to that described for spin systems A and B above, concerted interpretation of the HMQC, HMBC, and ROESY spectra quickly led to the assembly of additional structural subunits of the molecule. Spin system C is shown by **8**, spin system D by **9**.

SUBSTRUCTURE B.—Given the two structural fragments shown by **8** and **9**, we began the process of assembling them into a more complete structural component. We observed that one nitrogen-bearing carbon in spin system D resonated at 140.9 ppm. An rOe was observed to the protons resonating at 7.239 and 8.035 ppm from the *N*-Me group resonating at 3.952 ppm. A long-range heteronuclear connectivity was observed

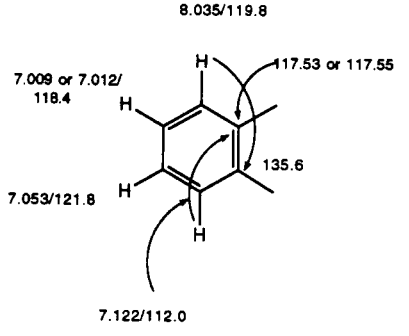

8

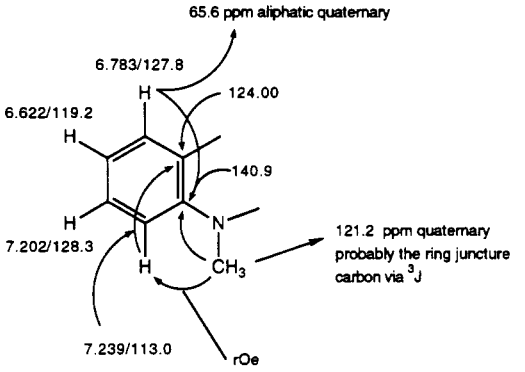

9

in the HMBC spectrum from the *N*-Me group to a quaternary carbon resonating upfield at 121.2 ppm. The 121.2 ppm carbon also exhibited a long-range correlation to the 8.035 ppm proton, implying the construction of a substructural fragment similar to that established by **5**. The chemical shift of the 121.2 ppm quaternary carbon, in analogous fashion, required the presence of a nitrogen atom beta to it. Since we had used three of the four nitrogen atoms, the remaining nitrogen was that of an indole. In particular, the proton resonating downfield at 10.669 ppm appeared as a doublet ($^1J_{NH} = 66$ Hz) when a ^{15}N satellite spectrum was recorded, confirming that this resonance arises from an indole NH. Long-range connectivities in the HMBC spectrum from the 10.669 ppm proton were also observed to the 121.2 ppm quaternary carbon and to one of the two nearly overlapped quaternary carbons resonating near 117.5 ppm.

A ^{15}N HMQC spectrum was also recorded. A correlation was observed from the proton resonating at 10.669 ppm to a ^{15}N resonating at 118.9 ppm. The chemical shift of the cryptospirolepine [**2**] indole ^{15}N-10′ resonance compared favorably with the ^{15}N resonance chemical shifts of several indoloquinolizidine analogues and reserpine, which ranged from 117.9 to 119.6 ppm (21).

To this point, we had utilized all but two carbons in the assembly of the structural fragments that have been described. One of the two nearly overlapped quaternary carbons at ca. 117.5 ppm remained and was a reasonable chemical shift for the indole nitrogen-bearing carbon that can be assembled by attaching the 66.0 ppm quaternary carbon to this indole ring. This afforded an indoloquinoline quite similar to cryp-

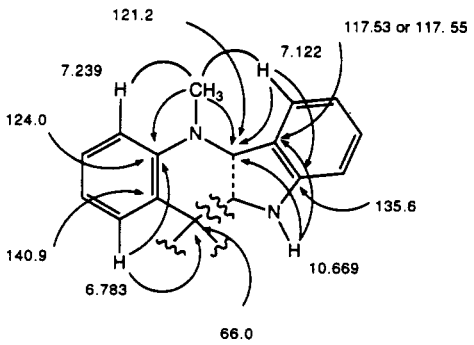

10

tolepine. The resultant structural fragment was also in agreement with the ms data because it has a mass of 232. Moreover, because the 6.273 ppm proton of the other portion of the molecule exhibited a connectivity to the 66.0 ppm quaternary carbon, we had established the point through which two portions of the molecule are linked. This series of deductions gave **11**.

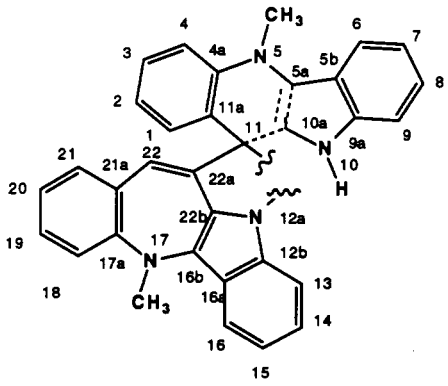

11

All that remained to be incorporated into the structure at this point was the quaternary carbon resonating at 188.4 ppm and one oxygen. Based on chemical shift, the 188.4 ppm resonance arises from a carbonyl. No connectivities were observed to the 188.4 ppm carbon in any HMBC spectrum nor in any SIMBA spectra acquired with a series of optima for this resonance. Unfortunately, an attempt to acquire a SELINADEQUATE spectrum by selective excitation of the spiro C-1/C-11′ resonance was also unsuccessful. However, by attaching the carbonyl to the remaining valence position of the 66.0 ppm quaternary carbon and bridging to the indole nitrogen of the bottom portion of the molecule, we completed the structure, giving **2**, for which we have proposed the name cryptospirolepine.

Although the assembly of the structure of cryptospirolepine [**2**] was completed, there remained the ambiguity in the assignment of the protons at the 5 and 7′ positions, which correspond to the protons resonating at 7.009 and 7.012 ppm (see structures **4** and **8**, respectively). The unequivocal assignment of these resonances was made by the identification of the carbon resonances vicinal to C-4 and C-6′ from an HMQC-TOCSY spectrum (27) using the method described in the recent review of Martin and Crouch (28). Thus, C-5 was assigned as the carbon resonating at 126.19 ppm and C-7′ was assigned as the carbon resonating at 118.35 ppm. Given these carbon assignments, H-5 and H-7′ were differentiated from an HMQC spectrum zero-filled to 2048 points in the proton (F_2) frequency domain and were assigned as 7.012 and 7.009 ppm, respectively. Complete ^1H and ^{13}C chemical shift assignments for cryptospirolepine [**2**] are given in Table 2.

The proposed structure for **2** contains a tertiary amide group on the basis of nmr and ms data. Since strong absorption bands are generally observed for tertiary amides between 1700 and 1650 cm^{-1} (carbonyl stretching vibration, or $\nu_{c=o}$) (22), confirmation of this group was attempted using ir spectroscopy. Only one band was observed between 1600 and 1700 cm^{-1}. This moderately intense band was observed at 1612 cm^{-1} and lies within the region where aromatic ring stretching vibrations rather than tertiary amide $\nu_{c=o}$ modes usually occur. Furthermore, the modest intensity of this band is more typical of one involving an aromatic ring stretching vibration rather than

TABLE 2. ^{1}H and ^{13}C Resonance Assignments for Cryptospirolepine [2] in DMSO-d_6. (Data were recorded at proton observation frequencies of either 399.952 or 499.843 MHz.)

Position	Chemical shifts δ (ppm)		
	^{1}H	^{13}C	^{15}N[a]
1/11′		66.0	
2		188.4	
3			
3a		139.9	
4	6.613	111.5	
5	7.012	126.2	
6	7.059	120.1	
7	8.324	123.0	
7a		117.8	
7b		123.4	
8-*N*Me	4.365	36.2[b]	
8a		138.5	
9	8.004	116.1	
10	7.827	131.4	
11	7.459	122.1	
12	8.400	125.6	
12a		116.8	
13	6.273	93.2	
13a		137.3	
13b		120.4	
1′	6.783	127.8	
2′	6.622	119.2	
3′	7.202	128.3	
4′	7.239	113.0	
4a′		140.9	
5′-*N*Me	3.941	36.2[b]	
5a′		121.2	
5b′		117.53[c]	
6′	8.035	119.8	
7′	7.009	118.3	
8′	7.053	121.9	
9′	7.122	112.0	
9a′		135.6	
10′	10.669		118.9
10a′		117.55[c]	
11′		66.0	
11a′		124.0	

[a] ^{15}N chemical shifts are reported in ppm downfield from HNO_3.
[b,c] Values with the same superscript may be transposed.

an amide carbonyl stretching mode. Given the high degree of aromaticity of **2**, the solid state ir data were considered insufficient for assigning this band to a $\nu_{c=o}$ mode. Consequently, its behavior in several different solvent systems was examined; the results of these studies confirmed that the 1612 cm^{-1} band arises from a $\nu_{c=o}$ mode.

In the first solution study, the effect of hydrogen bonding on the position of the proposed carbonyl band at 1612 cm^{-1} was tested. This was achieved by dissolving the compound in both MeCN-d_3 and MeOH-d_4–MeCN-d_3 (2:3) and taking ir spectra of these solutions. A band observed at 1625 cm^{-1} in MeCN shifted to 1621 cm^{-1} in the mixed solvent. Since the solvent containing MeOH has the capacity to form intermolecular hydrogen bonds with proton acceptor groups like carbonyls (-OH · · ·

O=C), the frequency shift in the mixed system is attributed to hydrogen bond formation. The magnitude (4 cm^{-1}) and direction (to lower wavenumber) of this shift are consistent with the behavior expected for a carbonyl group.

In the second study, the effect of solvent polarity on the frequency of the bands in the double bond stretching region above 1600 cm^{-1} was studied for solutions of **2** in DMSO-d_6 and MeCN-d_3. Both of these solvents are net hydrogen bond acceptors, but DMSO is appreciably more polar and would be expected to produce a larger shift in the position of bands arising from vibrational modes involving polar moieties like amide carbonyls. Conversely, if the band at 1612 cm^{-1} is due to an aromatic C=C ring stretching mode, polarity-induced band shifts should be small. As mentioned in the earlier solvent study, the band at 1612 cm^{-1} shifted to 1625 cm^{-1} in MeCN. This frequency is still within the range where aryl ring stretching modes can occur (up to 1625 cm^{-1}) and below the region where tertiary amides usually absorb (1700–1630 cm^{-1}). However, the band at 1612 cm^{-1} shifted significantly in DMSO, where a single, broad band was observed at 1664 cm^{-1}. This band lies well outside the region where aromatic ring stretching occurs, confirming that a carbonyl stretching vibration rather than an aryl ring stretching mode is responsible for the 1612 cm^{-1} band in the ir spectrum. Additionally, the 1612 cm^{-1} band shifted into the range where tertiary amides typically absorb (1700–1650 cm^{-1}), providing supportive evidence that a tertiary amide functionality is indeed present in **2** (22).

Having established the structure of cryptospirolepine [**2**] from the 2D nmr studies described above, we redirected our attention to the fragment ions observed in the fabms. Several fragment ions were observed between *m/z* 230 and 275, which further support the proposed structure of **2**.

The CAD (collisionally activated decomposition) daughter ion mass spectrum of the protonated molecular ion at 505 Da was obtained at both high energy (7 kV) and low energy (20 eV). The former spectrum was obtained using first-field region collisional activation and linked scanning at constant B/E. The low energy CAD mass spectrum was obtained using a hybrid mass spectrometer of BEqQ design. Both spectra showed similar fragmentation patterns although the relative ion intensities differed. Ions at 487, 445, 413, and 321 Da were most likely due to background ions from the glycerol. Ions at 487 and 445 Da represented the loss of H_2O and $HOCH_2CHO$, respectively, and arose from the fragmentation of clustered glycerol oligomers. Ions at 412 and 321 Da represented successive losses of glycerol from the matrix contribution of the 505 Da ion. There were no high energy fragmentation processes in the B/E scan that could further support the proposed structure of cryptospirolepine [**2**]; therefore all further work was performed using low energy CAD ms/ms techniques. The ion at 477 Da was due to the loss of CO from the protonated molecular ion of **2** and can be explained by a variety of pathways, all of which result in an even electron ion containing a preferred tertiary carbonium ion. This was the only low molecular weight loss that would be expected for the structure proposed for cryptospirolepine [**2**]. The major daughter ions, which were also observed in the fab mass spectrum, occurred at 233, 245, 259, and 273 Da; ms/ms spectra of these ions were obtained to further confirm the structure for cryptospirolepine as proposed by the nmr and hrms data.

The low-energy ms/ms daughter ion spectrum of 259 Da was acquired using the BEqQ configuration and a magnetic sector resolution of 1000. While there were many ions present, only a few were fragment ions of cryptospirolepine; the rest were background ions from the glycerol matrix. To illustrate this point, the magnetic sector resolution was increased to 5500 and only the portion of the 259 Da ion due to cryptospirolepine was allowed to enter the quadrupole (see Figure 1 for peak shape). The resulting daughter ion mass spectrum showed only ions at 217, 231, 243, and 259 Da as

compared to the ms/ms spectrum of 259 at 1000 resolution, which contains a series of ions which are due to glycerol matrix besides those ions resulting from fragmentation of the cryptospirolepine-derived 259 Da ion. The ion at 217 Da was observed in the daughter ion mass spectra for *m/z* 245 and 273; the ions at 231 and 243 were not observed in those spectra. The loss of 28 Da to yield 231 Da may be the loss of CH_2N, a radical from an *N*-Me with concurrent hydrogen rearrangement. However, this loss appears in the daughter ion mass spectra of ions whose structures involve the seven-membered azepine ring and may occur because of strain in the fused 7.5.5 section of the molecular structure. Loss of 16 Da to yield 243 Da would normally denote the loss of oxygen as for nitroso, nitro, and sulfone moieties. However, high-resolution mass measurement of *m/z* 259 showed that it does not contain oxygen. Thus the loss of a methyl group followed by the loss of a hydrogen or the loss of methane are the only two possible explanations for the loss of 16 Da. Furthermore, the parent ion mass spectrum of 259 Da showed that it arose directly from the protonated molecular ion of cryptospirolepine [**2**] and that no intermediate fragmentation was involved. Unfortunately, a structure cannot be proposed for the 259 Da ion based on the high resolution data, the daughter ion spectrum, and the parent ion mass spectrum.

The ms/ms daughter ion mass spectrum of the ion at 273 Da contained fragment ions at 258, 245, and 230 Da representing the loss of a methyl group, a CO molecule, and a CO molecule and methyl group, respectively. The daughter ion at 217 Da was an unknown fragment ion that may result from the loss of CO followed by the loss of a radical CH_2N with a one-hydrogen rearrangement as discussed for the *m/z* 259 ion. The

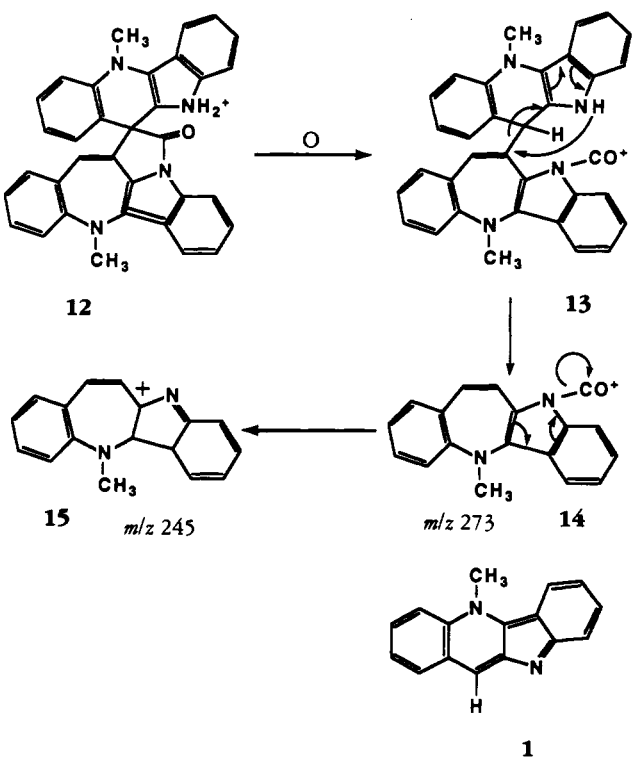

FIGURE 8. Fragmentation scheme showing the origin of the *m/z* 273 and 245 fragment ions from protonated cryptolepine [**12**] involving fragmentation at the spiro center.

217 Da ion was also present in the ms/ms daughter ion spectrum of the ion at 245 Da. The structure of the ion at 273 Da was assigned as **14** based on the observed ms/ms daughter ion spectrum and the elemental composition of $C_{18}H_{13}N_2O$ from the high-resolution data (see Table 1). A parent ion scan (a linked scan at constant B^2/E) showed that 273 arises only from the 505 Da ion, which suggests that the fragmentation of the spiro-unsaturated carbon is a process arising from the steps shown in Figure 8 where the neutral fragment is cryptolepine [**1**].

The structure for the ion at 245 Da was assigned as **15**. The ms/ms daughter ion spectrum of this exhibited several peaks due to glycerol matrix ions. However, the ions observed in this spectrum at 217 and 230 Da derive from fragments of cryptospirolepine [**2**]. The loss of an Me group from 245 yielded 230, whereas the ion at 217 Da could be rationalized through the loss of a CH_2N radical and a hydrogen rearrangement noted earlier for the 273 Da ion. The parent ion spectrum of *m/z* 245 showed that it arose only from 273 Da by the loss of CO. There is no other fragmentation pathway for this ion.

The structure of the ion at 233 Da can be assigned as **18** based on the ms/ms daughter ion mass spectra of the protonated molecular ion of cryptolepine [**1**] and the 233 Da ion of cryptospirolepine [**2**]. Both mass spectra were acquired at 120 eV collision energy and are identical. The structure of cryptolepine [**1**] has been unequivocally established in several previous studies (9,18). The parent ion spectrum of 233 Da showed that it arose only from the protonated molecular ion at 505 Da and that no intermediate ion fragment was involved. Rearrangement of the 505 Da ion may be involved in the formation of the 233 Da ion. A possible pathway for production of *m/z* 233 involves the protonation of cryptospirolepine at the *N*-Me group to give **16** followed by rearrangement to **17**, as shown in Figure 9. Fragmentation can then give **18** (*m/z* 233); it is probable that the structure of the leaving neutral portion involves a loss of CO followed by rearrangement of the five- and seven-membered rings.

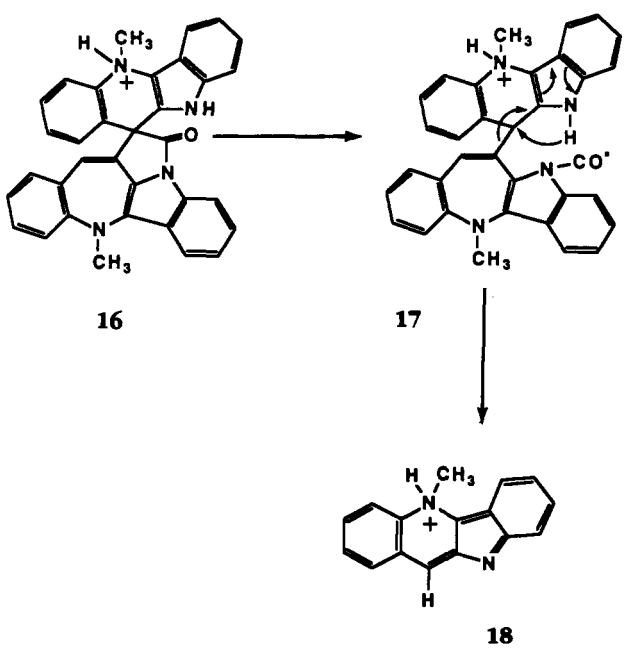

FIGURE 9. Fragmentation scheme showing a plausible mechanism for the fragmentation of the protonated molecular ion of cryptospirolepine [**2**] to give the 233 Da fragment ion.

EXPERIMENTAL

GENERAL EXPERIMENTAL PROCEDURES.—Mp's were determined on a Fisher-Johns apparatus and are reported uncorrected. The uv spectra were taken on a Perkin-Elmer Model 552A spectrophotometer in MeOH. Cc utilized Si gel or neutral Al_2O_3; tlc was over Si gel with the system C_6H_6-Me_2CO-NH_4OH (10:10:0.1). All solvents were evaporated under reduced pressure at 40°.

PLANT MATERIAL.—The plant material of *Cr. sanguinolenta* used in this study was collected at the Centre for Scientific Research into Plant Medicine, Mampong-Akwapim, Ghana in 1990 and was identified by Professor G.L. Boye of the Centre. An herbarium specimen is on deposit at the Centre.

EXTRACTION AND ISOLATION.—Powdered, oven-dried (60°) roots of *Cr. sanguinolenta* (1 kg) were defatted with petroleum ether for 12 h. The marc was extracted by percolation with EtOH (80%, 2 × 2 liters). The extract residue was thoroughly mixed with HOAc (10%, 500 ml), diluted with H_2O (500 ml), and allowed to stand overnight. The mixture was filtered, affording a clear solution (filtrate A) and some insoluble material. The aqueous acid-insoluble material was dissolved in a minimum amount of EtOH, treated with HOAc (10%, 200 ml), and diluted with H_2O until resinous material failed to precipitate. The resulting mixture was filtered, and the clear filtrate (filtrate B) was added to filtrate A. The combined aqueous filtrates were alkalinized with NH_4OH to pH 9.5 and extracted with $CHCl_3$ (5 × 200 ml). The combined $CHCl_3$ extractives were partitioned with H_2O (1 liter), dried over anhydrous Na_2SO_4, filtered, and evaporated to afford a dark alkaloidal residue (15 g).

The alkaloidal residue was dissolved in $CHCl_3$ (50 ml), adsorbed onto Al_2O_3 (20 g), and chromatographed over Al_2O_3 (200 g, column A). Elution was conducted with petroleum ether-$CHCl_3$ (1:2) followed by $CHCl_3$ and then $CHCl_3$-EtOH (9:1).

Elution of column A with $CHCl_3$ (1 liter) afforded a residue, which on treatment with absolute EtOH gave light brownish pink crystals of cryptospirolepine [**2**] (40 mg): quickly charring on heating; R_f 0.65; uv λ max (MeOH) 506 nm (log ε 4.44), 474 (4.19), 368 (4.38), 352 (sh) (4.27), 280 (4.65), 250 (4.80), 223 (sh) (4.75), 215 (4.83); (0.01 N methanolic NaOH) 506 (4.31), 474 (3.98), 390 (sh) (3.59), 341 (sh) (3.95), 327 (sh) (3.98), 311 (sh) (4.11), 282 (4.21), 252 (4.54); (0.01 N methanolic HCl) 470 (3.78), 375 (4.45), 278 (4.64), 246 (4.41), 223 (4.61); ir ν max (film, KBr) cm^{-1} 1612, 1588, 1512, 1454, 1394, 1326, 1305, 1228, 1051, 1025, 1008, 741 (additional details are presented in the ir experimental description below).

Elution of column A with $CHCl_3$-EtOH (9:1) gave a violet residue which was dissolved in $CHCl_3$ (50 ml). Addition of aqueous EtOH (60%, 50 ml) followed by heating and cooling to room temperature afforded long violet needles of cryptolepine [**1**] (4.84 g), mp 166–167°; R_f 0.0, identical to an authentic sample (8,18) by direct comparison (uv, ir, nmr, and ms).

Fabms was performed on a VG 70SQ mass spectrometer equipped with a FAB 11NW Saddle Field Ion Gun from Ion Tech, Ltd. Xenon was used as the bombardment gas at a pressure of 1×10^{-6} torr in the mass spectrometer ion source and a FAB Gun current of 1 milliamp at 7 kV. Low energy ms/ms experiments were conducted at collision energies of 10–500 eV using the quadrupole sector of the EBqQ design of the VG 70SQ. Air was used as the collision gas at a pressure of 5×10^{-5} torr in the RF-only first quadrupole sector. High-energy ms/ms experiments were conducted at a collision energy of 7 kV using first-field region linked scanning methods. The collision gas was air at a pressure in the collision cell, which reduced the primary beam intensity by 50 percent. Fab hrms measurements were conducted at a 7500 resolution (10% valley definition) using multichannel analysis software peak matching techniques.

All nmr spectra were recorded on a 3-mg sample of **2** dissolved in 600 μl of DMSO-d_6 on either a Varian Unity 400 or a Varian VXR-500S spectrometer. Both instruments were equipped with Z·Spec® indirect detection probes obtained from Nalorac Cryogenics Corporation, Martinez, CA. Observation frequencies for protons were 399.952 or 499.843 MHz, respectively. Typical 90° proton pulse widths were 10.8 and 12.6 μsec, respectively.

The COSY spectrum of cryptospirolepine [**2**] was recorded at 400 MHz using the pulse sequence and phase cycling of Bax *et al.* (23). Data were acquired as 1024 × 256 points with a spectral width of 1087 Hz in both frequency domains and with a total of 8 transients/t_1 increment. The data were sine-bell apodized, zero-filled to 2048 × 2048 points during processing, and symmetrized (24) prior to plotting. A relayed COSY (RCOSY) spectrum (not shown) was also recorded using the method of Eich *et al.* (25) using a relay period (tau) of 60 msec.

Heteronuclear chemical shift correlation data were obtained at 500 MHz by inverse-detection for reasons of sensitivity using the pulse sequence of Bax and Subramanian (26). The spectrum was acquired as 384 × 120 points with spectral widths of 1047 and 9052 Hz in F_2 and F_1, respectively. The data were processed using Gaussian apodization prior to both Fourier transforms and were zero-filled to 1024 × 512 points.

Heteronuclear chemical shift correlation data with relayed coherence transfer were acquired using a

modification of the HMQC-TOCSY pulse sequence originally described by Lerner and Bax (27). Rather than delaying the onset of broadband heteronuclear decoupling by the interval $\frac{1}{2}J$, as in the original work of Lerner and Bax, which suppresses the direct responses, we elected instead to initiate decoupling with the commencement of acquisition to retain the direct responses as described in the recent review of Martin and Crouch (28).

SIMBA spectra were recorded using the pulse sequence described by Crouch and Martin (20). The selective pulse applied to the individual ^{13}C resonances was a 12 msec Gaussian pulse followed by a 9 msec refocussing delay. A total of 12288 data points were acquired; these were zero-filled to 32K points during processing, which employed a combination of a negatively decaying exponential and a Gaussian function. The power spectrum was plotted and shown above a high-resolution reference spectrum in Figure 7.

HMBC spectra optimized for 10 Hz were recorded using the pulse sequence of Box & Summers (29). The HMBC spectrum of **2** is shown in Figure 6.

Ir spectra were acquired using an FX6260 FTIR spectrophotometer (Analect) equipped with a model FXA-501 beam condenser (9×). The interferometer was operated at 2 cm^{-1} resolution, and the ir signal was detected using a broadband MCT (mercury-cadmium telluride) detector.

Cryptospirolepine [**2**] was analyzed in the solid state as a KBr pellet (Aldrich 99+% KBr). Solutions were prepared for ir data acquisition by dissolving the sample in MeCN-d_3, MeOD-d_4–MeCN-d_3 (2:3), and DMSO-d_6 (MSD Isotopes). Spectra were taken of these solutions in a micro-cavity KBr cell (Spectra-Tech, Inc.) with a 0.1 mm (i.d.) cell path. Ir data were smoothed using the smoothing routine supplied with the Ft-ir instrument (9-point smoothing). Interference bands from solvents were removed by digital subtraction from the spectral data in the solution studies.

LITERATURE CITED

1. G.L. Boye and O. Ampofo, "Proceedings of the First International Symposium on Cryptolepine." Kumasi, Ghana, University of Science and Technology, 1983.
2. E. Clinquart, *Bull. Acad. R. Med. Belg.*, **12**, 6237 (1929).
3. E. Delvaux, *J. Pharm. Belg.*, **13**, 955, 973 (1931).
4. F. Fichter and R. Boehringer, *Ber.*, **39**, 3932 (1906).
5. F. Fichter and H. Probst, *Ber.*, **40**, 3478 (1907).
6. F. Fichter and F. Rohner, *Ber.*, **43**, 3489 (1910).
7. E. Gellert, Raymond-Hamet, and E. Schlittler, *Helv. Chim. Acta*, **34**, 642 (1951).
8. D. Dwuma-Badu, J.S.K. Ayim, N.I.Y. Fiagbe, J.E. Knapp, P.L. Schiff Jr., and D.J. Slatkin, *J. Pharm. Sci.*, **67**, 433 (1978).
9. S.Y. Ablordeppey, C.D. Hufford, R.F. Bourne, and D. Dwuma-Badu, *Planta Med.*, **56**, 416 (1990).
10. Raymond-Hamet, *C.R. Soc. Biol.*, **126**, 768 (1937); *Chem. Abstr.*, **32**, 2211 (1937).
11. Raymond-Hamet, *C.R. Soc. Biol.*, **207**, 1016 (1938); *Chem. Abstr.*, **33**, 8295 (1938).
12. K. Boakye-Yiadom, *Q.J. Crude Drug Res.*, **17**, 78 (1979).
13. K. Boakye-Yiadom and D. Dwuma-Badu, "Proceedings of the 3rd symposium on African Medicinal Plants," University of Ife, Ife-Ife, Nigeria, 1977.
14. K. Boakye-Yiadom and S.M. Heman-Ackah, *J. Pharm. Sci.*, **68**, 1510 (1979).
15. S.O.A. Bamgbose and B.K. Noamesi, "7th International Congress of Pharmacology," Abstr. No. 1289, Pergammon Press, NY, 1978.
16. B.K. Noamesi and S.O.A. Bamgbose, *Planta Med.*, **39**, 51 (1980).
17. S.O.A. Bamgbose and B.K. Noamesi, *Planta Med.*, **41**, 392 (1981).
18. A.N. Tackie, M.H.M. Sharaf, P.L. Schiff Jr., G.M. Boye, R.C. Crouch, and G.E. Martin, *J. Heterocycl. Chem.*, **28**, 1429 (1991).
19. R.L. Johnson and L.C.E. Taylor, *Org. Mass Spectrom.*, **22**, 807 (1987).
20. R.C. Crouch and G.E. Martin, *J. Magn. Reson.*, **92**, 189 (1991).
21. S.N.Y. Fanso-Free, G.T. Furst, P.R. Srinivasan, R.L. Lichter, R.B. Nelson, J.A. Panetta, and G.W. Gribble, *J. Am. Chem. Soc.*, **101**, 1549 (1979).
22. L.J. Bellamy, "The Infrared Spectra of Complex Molecules," Chapman and Hall, London, 1975, pp. 241–243.
23. A. Bax, R. Freeman, and G.A. Morris, *J. Magn. Reson.*, **42**, 164 (1981).
24. R. Baumann, G. Wider, R.R. Ernst, and K. Wüthrich, *J. Magn. Reson.*, **44**, 402 (1981).
25. G. Eich, G. Bodenhausen, and R.R. Ernst, *J. Am. Chem. Soc.*, **104**, 3731 (1982).
26. A. Bax and S. Subramanian, *J. Magn. Reson.*, **67**, 565 (1986).
27. L. Lerner and A. Bax, *J. Magn. Reson.*, **69**, 375 (1986).
28. G.E. Martin and R.C. Crouch, *J. Nat. Prod.*, **54**, 1 (1991).
29. A. Bax and M.F. Summers, *J. Am. Chem. Soc.*, **108**, 2093 (1986).

Received 22 April 1992